Three-dimensional tsunami runup simulation for the port of Koborinai on the Sanriku coast of Japan

Dong Chule Kim†, Kyeong Ok Kim‡, Efim Pelinovsky∞, Ira Didenkulova∞§, Byung Ho Choi+

† Technology R&D Institute
Hyein E&C Co., Ltd., Seoul 157-861, Korea
skkkdc@chol.com

‡ Marine Environments & Conservation Research Division, Korea Institute of Ocean Science & Technology, Ansan 426-744, Korea
kokim@kiost.ac

∞ Nizhny Novgorod State Technical University, Institute of Applied Physics, Nizhny Novgorod, and Special Research Bureau for Automation of Marine Research, Yuzhno-Sakhalinsk, Russia
pelinovsky@hydro.appl.sci-nnov.ru
ira@cs.ioc.ee

§ Institute of Cybernetics at Tallinn University of Technology, Tallinn, Estonia
ira@cs.ioc.ee

+ Dept. of Civil and Env. Engineering Sungkyunkwan University, Suwon 440-746,Korea
bhchoi.skku@gmail.com
*corresponding author

www.cerf-jcr.org

www.JCRonline.org

ABSTRACT

Kim, D.C., Kim, K.O., Pelinovsky, E., Didenkulova, I. and Choi, B.H., 2013. Three-dimensional tsunami runup simulation for the port of Koborinai on the Sanriku coast of Japan. *In:* Conley, D.C., Masselink, G., Russell, P.E. and O'Hare, T.J. (eds.), *Proceedings 12th International Coastal Symposium* (Plymouth, England), *Journal of Coastal Research*, Special Issue No. 65, pp. 266-271, ISSN 0749-0208.

The huge tsunami generated by the earthquake that occurred off the Pacific coast of Japan at 14:46 JST (05:46 UTC) on Friday, 11 March 2011 produced a maximum runup of 40 m on the east coast of Japan. The earthquake triggered extremely destructive tsunami waves up to 37.9 m in height that struck Japan minutes after the quake. Koborinai is a tiny fishery port located north of Miyako City in the Iwate Prefecture. A survey team from the University of Tokyo Earthquake Research Institute (ERI) found high water marks and other evidence of a gigantic wave at the port of Koborinai. The port is on low land sandwiched between two mountains. A joint survey team from ERI-Sungkyunkwan University (SKKU) and Korea Ocean Research & Development Institute (KORDI) visited again and surveyed the site in detail. The 3D Princeton Ocean Model was applied to describe the propagation and runup of the tsunami on the Japanese coast. The numerical simulation results obtained were in satisfactory agreement with observations made in the general area, except those made in many v-shaped valleys along the northern Iwate coast. The extremely high runup of tsunami waves at the port at Koborinai were successfully reproduced by numerical simulation through stepwise refinement of the spatial scale using multi-nesting and consideration of the vertical acceleration of flow along steep slopes using a CFD model to solve the Reynolds-averaged Navier–Stokes (RANS) equations. The velocity field was also computed, and the simulation results show that the water flow that climbed the coast possessed a strong vertical velocity component.

ADDITIONAL INDEX WORDS: *2011 East Japan Earthquake, tsunami numerical modeling, extreme runup*

INTRODUCTION

The huge tsunami generated by the earthquake that occurred off the Pacific coast of Japan at 14:46 JST (05:46 UTC) on Friday, 11 March 2011 (hereafter referred to as the 2011 East Japan earthquake) produced a maximum runup of 40 m on the east coast of Japan. The epicenter of the earthquake was approximately 72 km (45 miles) east of the Oshika Peninsula in the Tohoku area, and the hypocenter was located at an underwater depth of approximately 32 km. The earthquake triggered extremely destructive tsunami waves up to 37.9 m in height (the runup height) that struck Japan minutes after the quake, in some cases traveling up to 10 km inland, with smaller waves reaching many other countries after several hours. Tsunami warnings were issued and evacuations ordered along Japan's Pacific coast and the coasts of at least 20 other countries, including the entire Pacific coast of the Americas. Koborinai is a tiny fishery port located north of Miyako City in the Iwate Prefecture (Figure 1). A survey team from the University of Tokyo Earthquake Research Institute (ERI) found high water marks and other evidence of a huge wave at the port of Koborinai and reported that the local topography most likely contributed to the size of the wave. The port, located on low land sandwiched between two capes, is located on V-shaped incised valley with width of 300 m and steep slopes. Two small barriers intended to protect fishing boats were completely destroyed. A road exits circuitously from the harbor to the hill top. A joint survey team from ERI, Sungkyunkwan University (SKKU) and Korea Ocean Research & Development Institute (KORDI) visited again and surveyed the site in detail using non-prism Total Station equipment. Figure 2 shows photos of the damaged port of Koborinai from an elevated perspective. A detailed report of the field survey of this area is presented in (Tsuji et al, 2011). Such unexpectedly high tsunami waves may have been caused in part by the terrain, as has been shown with previous earthquake events: V-shaped valleys on the west coast of Okushiri Island experience surprisingly high tsunami runups after the 1993 Hokkaido earthquake (Satake and Tanioka, 1995; Shuto and Matsutomi, 1995), as did the Lhok Nga twin hills after the

DOI: 10.2112/SI65-046.1 received 07 December 2012; accepted 06 March 2013.

2004 Sumatra–Andaman earthquake (Lavigne et al., 2009; Paris et al., 2009).

The goal of this study was to reproduce the tsunami phenomena that occurred at the Koborinai Port after the 2011 East Japan earthquake within the framework of a quasi-3D shallow-water model and fully nonlinear dispersive Reynolds-averaged Navier–Stokes (RANS) models.

TSUNAMI SOURCE MODEL

The genesis of the 2011 East Japan earthquake tsunami is well described by the seismic finite fault model (FFM) developed by the United States Geological Survey (USGS). The earthquake parameters were computed using Global Seismographic Network (GSN) broadband waveforms downloaded from the National Earthquake Information Center (NEIC) waveform server, and teleseismic broadband P waveforms, broadband SH waveforms, and long-period surface waves were selected for analysis. The waveforms were first converted to displacements by removing the instrument response and then were used to constrain the slip history based on a finite fault inverse algorithm. The fault planes were defined using the updated W-phase moment tensor solution of NEIC, adjusted to match local slab geometry (Hayes, 2011). The fault was composed of subfaults of 25 grids of 25 km along the strike direction and 13 grids of 20 km in the downdip direction. Each subfault was characterized by its slip distance, rake, strike, dip angles, and time of rupture and rise.

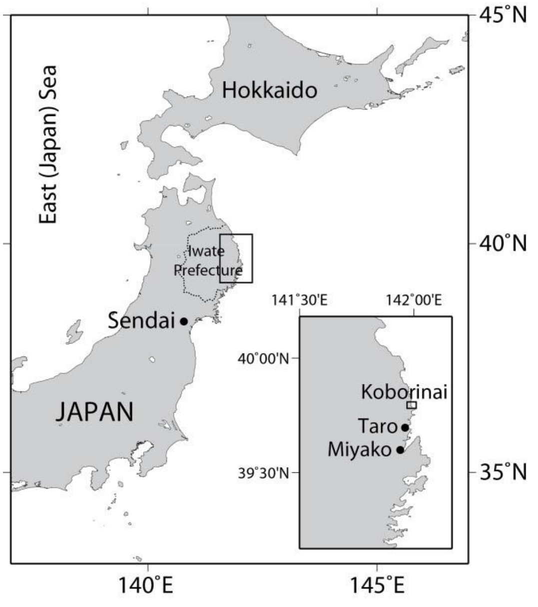

Figure 1. The location of the port of Koborinai.

Figure 2. Photos of the port of Koborinai from a top perspective.

The values of other fault parameters determined by the inverting method using buoy observations (NOAA; Wei et al, 2012) were compared with values determined by the USGS. The 6 subfaults were pre-computed units (Gica et al, 2008) to facilitate a rapid inversion process.

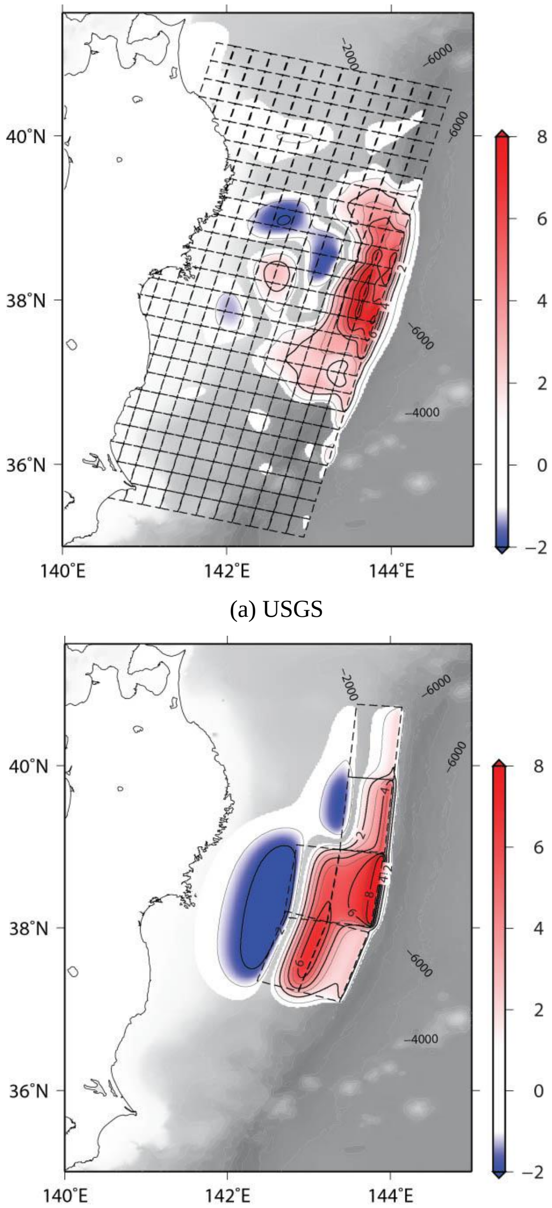

(a) USGS

(b) NOAA

Figure 3. The vertical component of water deformation (meters) computed using Okada's solution.

Water displacements at the tsunami sources were estimated using Okada's solution (1985) and are shown in Figure 3. The initial elevation and velocity were assumed to be zero. The water deformation at each sub-fault was forced to an additional water elevation in every time step during the rise time from the rupture time. Time information obtained from the United States National Oceanic and Atmospheric Administration (NOAA) was used and is shown in Table 1 along with other parameters. The water deformation (ΔU) is composed of the vertical displacement (Uz) and the vertical movement (Uh) converted by horizontal movement (Ux, Uy) of the bottom (H) slope.

$$\Delta U = Uz + Uh$$

$$Uh = -Ux\frac{\partial H}{\partial x} - Uy\frac{\partial H}{\partial y}$$

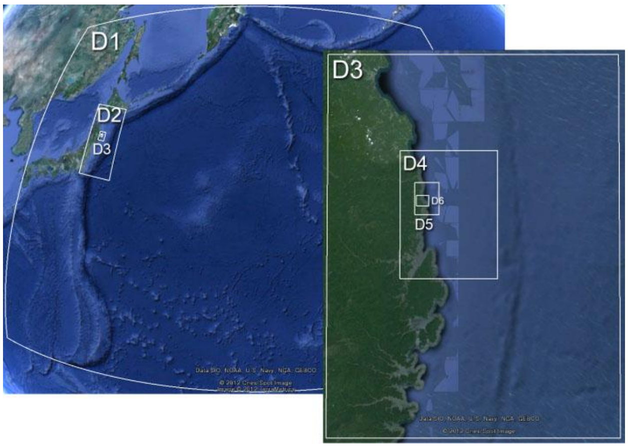

Figure 4. Nested grid system of the finite difference tsunami model.

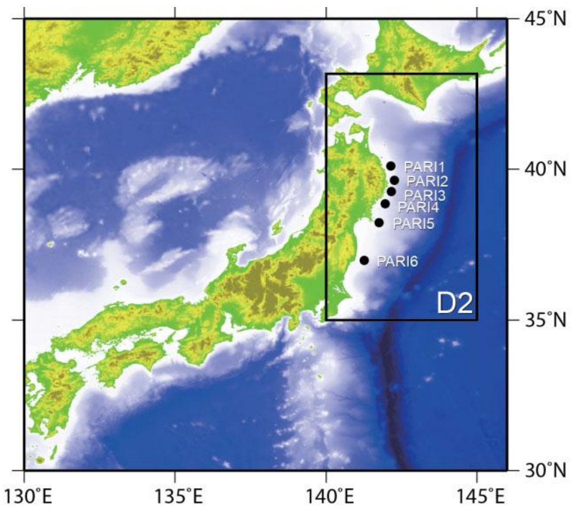

Figure 5. Six GPS wave buoys (black dots). The black square box indicates the second domain (D2).

Table 2. Information of grid and nesting systems

Domain	NX	NY	DX DY (arc-sec)	DT (sec)	Nesting ratio	Comp Mode
D1	2100	1260	120	10		2D
D2	600	980	30	2.5	1:4	3D
D3	360	360	10	1.0	1:3	3D
D4	360	360	3.33	0.5	1:3	3D
D5	270	270	1.11	0.1	1:3	3Dwad
D6	405	270	0.37	0.05	1:3	3Dwad

TSUNAMI PROPAGATION MODEL

The well-known finite difference Princeton Ocean Model was applied in this study to simulate tsunami wave propagation during the 2011 East Japan event. The details of this model are not discussed in this paper.

Six sub-regions (Figure 4) in total, all of which had different grid sizes, were used in the tsunami propagation model. The first domain (D1) was computed in depth-averaged (2D) mode and the other domains were computed in 3D mode with 10 vertical sigma levels. The radiation open boundary scheme was employed for the first domain (D1), and the simple one-way nesting scheme was employed for the other domains by interpolating the water elevation and current values from the mother domain. The boundary condition of the internal model in the second domain (D2) employed the radiation scheme because the 3D current input is not available for the mother domain, which was calculated in 2D mode. The largest domain (D1) had a 2100 x 1260 mesh system with a 2-minute grid resolution and a time step of 10 sec for trans-ocean propagation. The sub-domains were nested using 1:3 or 1:4 grid interpolations. The smallest domain (D6) had a 405 x 270 mesh system with a grid resolution of approximately 10 m and a time step of 0.05 sec. The "land" boundary conditions were assumed to be fully reflected in the last sea grids from D1 to D4 with a minimum water depth of 10 m. The runup of tsunami waves in domains D5 and D6 was computed using the wet-and-dry scheme proposed by Oey (2005). Table 2 shows information on the grid and nesting systems for all the domains. The bathymetry data are composed by GEBCO (Jones, 2003). Bathymetry (50-meter-resolution) data and topographic (10-meter-resolution) data were obtained from the Japanese Government (Central Disaster Management Council, 2003) and GSI (Geospatial Information Authority of Japan, http://fgd.gsi.go.jp/download/). Computed water elevations using two tsunami sources (USGS and NOAA) were compared with Global Positioning System (GPS) buoy records (Takahashi et al, 2011) in Figure 6.

Figure 7 show the topography heights and spatial distributions of the maximum water elevations due to tsunami runup in the last domain of POM (D6). The tsunami wave computed by the hydrostatic model could not reach 5 of the survey points.

Table 1. Fault parameters of the 2011 East Japan earthquake (modified from Wei et al., 2012)

Subfault	Latitude (°N)	Longitude (°E)	Length (km)	Width (km)	Depth (km)	Slip (m)	Rake (deg)	Strike (deg)	Dip angle (deg)	Rupture time(sec)	Rise time (sec)
A	40.3125	143.5273	100	47	5	4.66	90	185	19	250	30
B	39.4176	143.4246	100	47	5	12.23	90	185	19	250	30
C	38.5254	143.2930	100	47	5	21.27	90	188	19	130	30
D	38.5837	142.7622	100	47	21.28	26.31	90	188	21	155	30
E	37.6534	143.0357	100	47	5	4.98	90	198	19	10	30
F	37.7830	142.5320	100	47	21.28	22.75	90	198	21	10	30

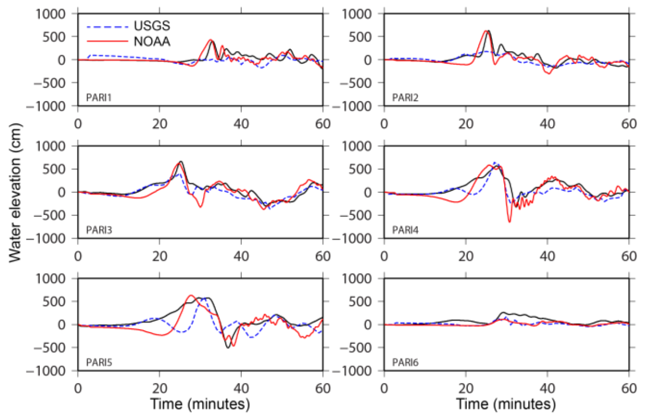

Figure 6. Comparison of computed and observed tsunami records.

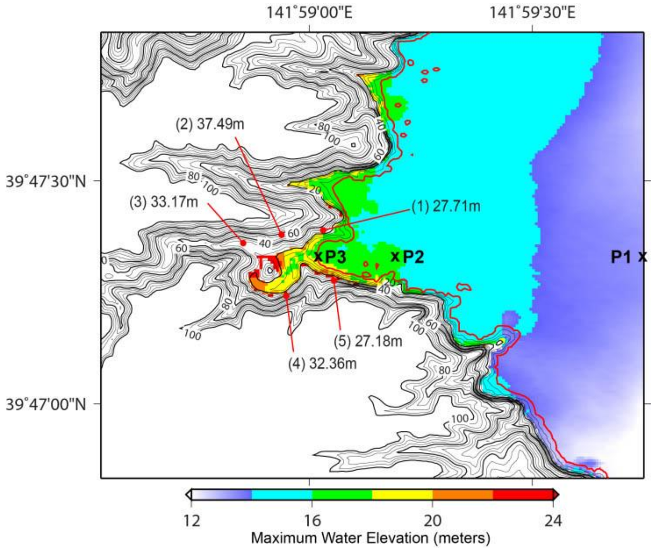

Figure 7. Spatial distribution of the maximum tsunami amplitudes (according to POM) and the surveyed runup heights.

3D COMPUTATIONS OF TSUNAMI WAVES AT THE PORT OF KOBORINAI

The FLOW3D code (Flow Science, 2002) was used to compute the tsunami characteristics at the Koborinai Port with high accuracy. FLOW3D solves fully nonlinear dispersive Navier–Stokes equations by the finite difference method. It utilizes a true volume-of-fluid (VOF) method to compute free surface motion and the fractional area/volume obstacle representation (FAVOR) technique to model complex geometric regions. To describe turbulence in a viscous fluid, a version of the k-model, updated with the help of renormalization group analysis, was used. This FLOW3D code has already been used to simulate tsunami waves (Choi et al., 2007, 2008ab) and to study solitary wave transformation over a step (Pelinovsky et al, 2010).

It is somewhat difficult to apply boundary conditions in FLOW3D because this model accepts only a single time-dependent boundary variable. Thus, a representative boundary point was selected from the sixth domain of the POM model (P1 in Figure 7). Figure 8 shows the water elevation and horizontal velocity used for boundary forcing. A slow negative surge of 3 m was computed starting from 15 minutes after the earthquake and continuing for nearly 30 minutes, until before the first wave. The first crest had maximum amplitude of 13 m. The second and third crests followed at approximately 6-minute intervals. The water flowed mainly from east to west.

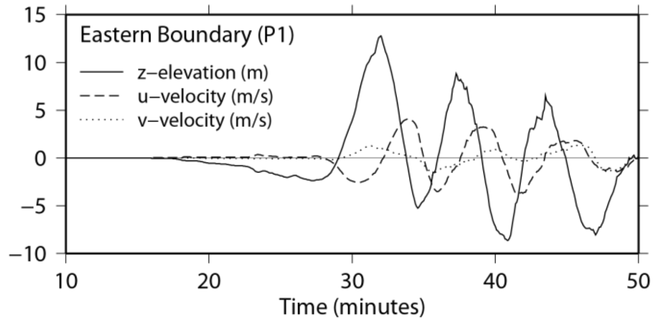

Figure 8. Time series of the water elevation and horizontal velocity of the boundary condition at the east-side boundary (P1).

Table 3. Comparison of observed and computed runup heights at Koborinai

Site No.	Observed height (E.L., m)	POM3D*	Flow3D
1	27.71	19.81	28.74
2	37.49	21.34	31.27
3	33.17	24.62	34.33
4	32.36	20.22	33.29
5	27.18	28.37	26.83

* The nearest inundation height if the site is not inundated

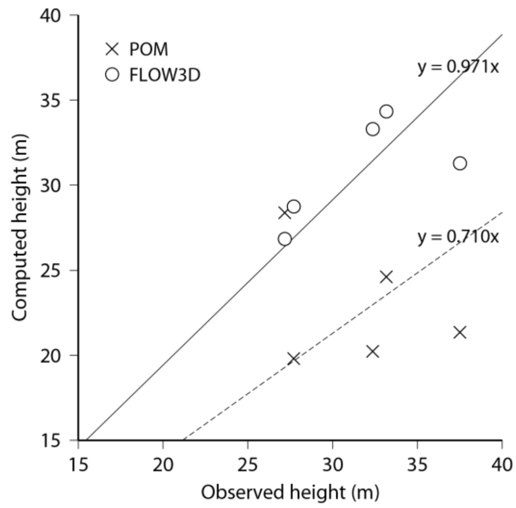

Figure 9. Comparison between observed and computed runup heights at Koborinai

The observed and computed runup heights are shown in Table 3 and Figure 9. Where the computed runups obtained from POM were not matched at the survey points, the nearest inundation heights were compared with observation heights. The correlation obtained with POM was 0.71 but a higher correlation (0.97) was obtained with the FLOW3D model.

The direction of water flow is shown in Figure 10 by vectors of particle velocity. Water climbed to a height of more than 30 m in a narrow valley in the mountain behind the port. A comparison between the computed and observed runup heights is shown in Figure 10b for a time of 40.4 min. The maximum computed runup height was 34.33 m (at point #3), which is approximately 3 m less than the maximum observed runup height (37.49 m).

It is important to mention that the maximum slope angle in the valley is approximately 60°, which leads to large values of vertical velocity, which are usually ignored in depth-averaged models. Figure 11 shows that the velocity field reaches values of 3 m/s at T = 40 min. It is evident that large vertical velocities will occur in water flow climbing a steep slope. If we use a hydrostatic model, extreme runup heights will be underestimated, as illustrated by Figure 7, which shows that the wave height computed using POM is only 25 m.

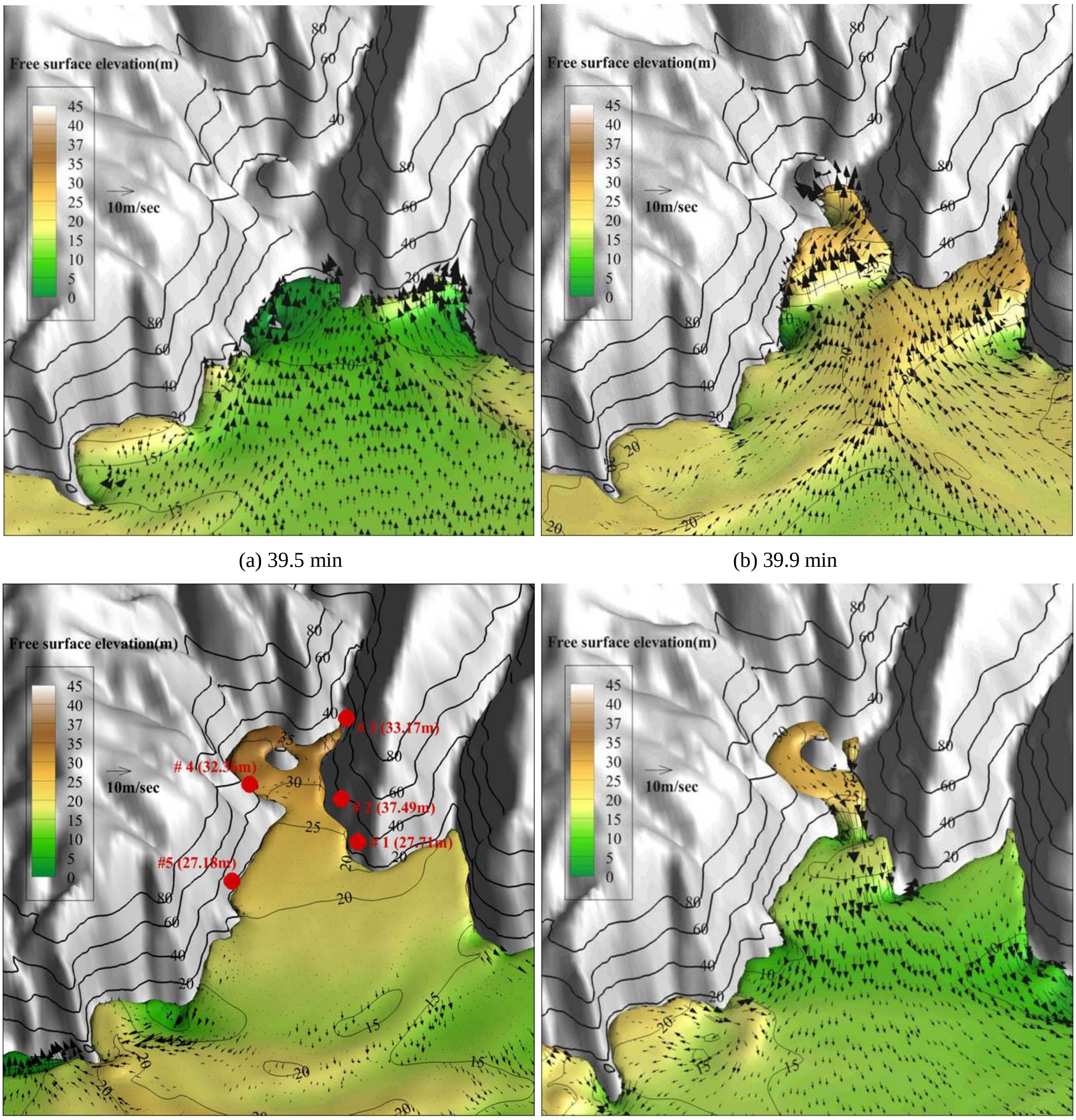

(a) 39.5 min (b) 39.9 min

(c) 40.4 min (d) 41.0 min

Figure 10. Snapshots of water elevation (contours) and resultant velocity (vectors) illustrating the tsunami running up and down the V-shaped valley.

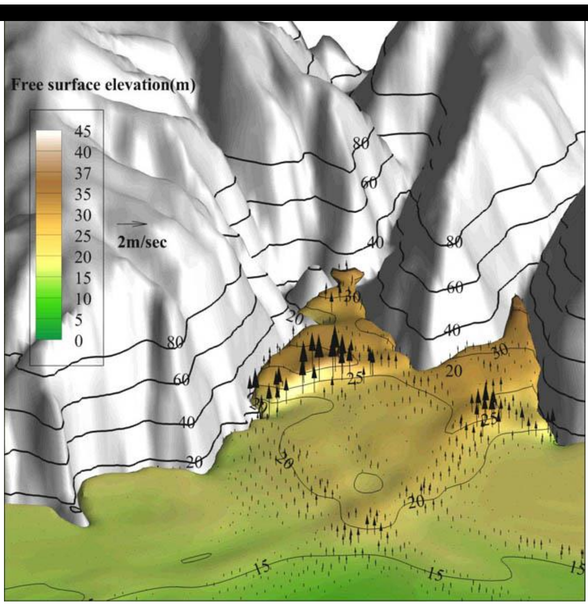

Figure 11. Zoomed image of water elevation (contours) and vertical velocity component (arrows) at T = 40 min.

CONCLUSIONS

The extreme runup height of 37.49 m observed at the Koborinai Port due to the 2011 East Japan earthquake tsunami was modeled numerically. In the first stage of tsunami propagation from the source to the coast, the Princeton Ocean Model was used. Computations were made for nested domains with different space and time step resolutions. The numerical simulation results are verified by tide-gauge observations in some Japanese ports. The wave runup at the Koborinai Port was studied with 3D fully nonlinear dispersive Reynolds-averaged Navier–Stokes equations solved by FLOW3D using very detailed bathymetry and land topography data.

The maximum value of the computed runup height for the entire computed domain was 34.33 m, which is close to the maximum observed value of 37.49 m. The importance of considering 3D non-hydrostatic effects for waves climb steep slopes is demonstrated by the simulation results. When this effect is ignored, the computed heights do not exceed 10 m. Vertical velocities in the process of wave climbing on a coast can reach 3 m/s or more. Thus, 3D non-hydrostatic numerical models are suggested for use in prediction of tsunami characteristics on steep coasts and for estimation of the tsunami risk for such extremely dangerous areas.

ACKNOWLEDGEMENTS

This study was partially supported by the major research project “The development of the marine environmental impact prediction system following the disastrous event” funded by KIOST and by the BK21 Program at Sungkyunkwan University. ID and EP have been particularly supported by the Federal Targeted Program "Research and educational personnel of innovation Russia" for 2009-2013” and grants (MK-1440.2012.5, SF0140007s11, ETF8870, RFBR11-05-00216 and RFBR12-05-33087).

LITERATURE CITED

Central Disaster Management Council, 2003. Report of the technical investigation committee on earthquakes in the vicinity of the Japan Trench. Cabinet Office, Government of Japan (in Japanese).

Choi, B.H., Kim, D.C., Pelinovsky, E. and Woo, S.B., 2007. Three-dimensional simulation of tsunami run-up around conical island. *Coastal Engineering*, 54, 618-629.

Choi, B.H., Pelinovsky, E., Kim, D.C., Didenkulova, I. and Woo, S.B., 2008a. Two- and three-dimensional computation of solitary wave runup on non-plane beach. *Nonlinear Processes in Geophysics*, 15, 489-502.

Choi B.H., Pelinovsky E., Kim D.C., Lee H.J., Min B.I. and Kim K.H., 2008b. Three-dimensional simulation of 1983 central East (Japan) Sea earthquake tsunami at the Imwon Port (Korea). *Ocean Engineering*, 35, 1545-1559.

Flow Science, 2002. *FLOW-3D User's Manual*.

Gica, E., Spillane, M., Titov, V.V., Chamberlin, C. and Newman, J.C., 2008. Development of the forecast propagation database for NOAA’s Short-term Inundation Forecast for Tsunamis (SIFT), NOAA Tech. Memo. OAR PMEL-139, 89 pp.

Hayes, G., 2011. Finite Fault Model, Updated Result of the Mar 11, 2011 Mw 9.0 Earthquake Offshore Honshu, Japan http://earthquake.usgs.gov/ earthquakes/eqinthenews/2011/usc0001xgp/finite_fault.php, 2011.

Jones, M.T., 2003. GEBCO Digital Atlas: Centenary Edition of the IHO/IOC General Bathymetric Chart of the Oceans [CD-ROM], Natl. Environ. Res. Counc., Swindon, U.K.

Lavigne, F., Paris, R., Grancher, D., Wassmer, P., Brunstein, D., Vautier, F., Leone. F., Flohic. F., de Coster, B., Gunawan, T., Gomez. C., Setiawan, A., Cahyadi, R. and Fachrizal, 2009. Reconstruction of tsunami inland propagation on December 26, 2004 in Banda Aceh, Indonesia, through field investigations. *Pure and Applied Geophysics*, 166, 259-281.

Oey, L., 2005. A wetting and drying scheme for POM. *Ocean Modelling*, 9, 133-150.

Okada, Y., 1985. Surface deformation due to shear and tensile faults in a half-space. *Bull. Seismol. Soc. Am.*, 75, 1135-1154.

Paris, R., Wassmer, P., Sartohadi, J., Lavigne, F. Barthomeuf, B., Deshgages, E., Grancher, D., Baumert, P., Vautier, F., Brunstein, D. and Gomez, C., 2009. Tsunamis as geomorphic crises: lessons from the December 26, 2004 tsunami in Lhok Nga, West Banda Aceh (Sumatra, Indonesia). *Geomorphology*, 104, 59-72.

Pelinovsky, E., Choi, B.H., Talipova, T., Woo, S.B. and Kim, D.C., 2010. Solitary wave transformation on the underwater step: theory and numerical experiments. *Applied Math Computations*, 217, 1704–1718.

Satake, K. and Tanioka, Y., 1995. Tsunami Generation of the 1993 Hokkaido Nansei-Oki Earthquake. *Pure and applied geophysics*, 144, 803-821.

Shuto, N. and Matsutomi, H., 1995. Field survey of the 1993 Hokkaido Nansei-Oki tsunami, *Pure and applied geophysics*, 144, 649-664.

Takahashi, S., Kuriyama, Y., Tomita, T., Kawai, Y., Arikawa, T., Tatsumi, D. and Negi, T., 2011. *Urgent survey for 2011 Great East Japan Earthquake and tsunami disaster in ports and coasts*, Technical Note of Port and Air Port Research Institute, No. 1231.

Tsuji, Y., Satake, K., Ishibe, T. Kusumoto, S., et al., 2011. Field Surveys of Tsunami Heights from the 2011 off the Pacific Coast of Tohoku, Japan Earthquake. *Bull. Earthquake Research Institute, University of Tokyo*, 86, 29-279 (in Japanese).

Wei, Y., Chamberlin, C., Titov, V.V., Tang, L. and Bernard, E.N., 2012. Modeling of the 2011 Japan Tsunami: Lessons for Near-Field Forecast. *Pure Appl. Geophys.*, DOI:10.1007/s00024-012-0519-z.